

Synthesis and Characterization of Three Novel Selenidohexacobalt Carbonyl Clusters. Crystal Structures of $[(\mu_3\text{-Se})\text{Co}_3(\text{CO})_7]_2\mu_4\text{-(Se}_2\text{)}$ and $\text{Co}_6(\mu_3\text{-Se})_8(\text{CO})_6\cdot 2\text{C}_6\text{H}_6$

G. Gervasio,*[†] S. F. A. Kettle,[‡] F. Musso,[†] R. Rossetti,[†] and P. L. Stanghellini*[†]

Dipartimento di Chimica Inorganica, Chimica Fisica e Chimica dei Materiali, Università di Torino, Via P. Giuria 7, 10125 Torino, Italy, School of Chemical Sciences, University of East Anglia, Norwich NR4 7TJ, England, and Department of Chemistry and Chemical Engineering, Royal Military College, Kingston, Ontario K7K 5L0, Canada

Received June 28, 1994[Ⓞ]

Reaction of dicobalt octacarbonyl with elemental red selenium at room temperature in THF solution gives rise to $\text{Co}_3(\text{CO})_9(\mu_3\text{-Se})$ (**1**), $\text{Co}_4(\text{CO})_{10}\mu_4\text{-(Se)}_2$ (**2**), $[(\mu_3\text{-Se})\text{Co}_3(\text{CO})_7]_2\mu_4\text{-(Se)}_2$ (**4**), and $\text{Co}_6(\mu_3\text{-Se})_8(\text{CO})_6$ (**5**). The complexes **4** and **5** have been characterized by a single-crystal X-ray diffraction analysis. Crystal data for **4** are as follows: triclinic space group $P\bar{1}$, $a = 9.649(2)$ Å, $b = 12.688(3)$ Å, $c = 12.952(6)$ Å, $\alpha = 66.61(3)^\circ$, $\beta = 71.89(3)^\circ$, $\gamma = 83.53(2)^\circ$, $V = 1383.1(8)$ Å³, $Z = 2$, $\rho(\text{calcd}) = 2.549$ Mg/m³. The structure was solved by direct methods and refined (1646 reflections, $F > 4.0 \sigma(F)$) to the final residuals $R = 0.084$ and $wR = 0.107$. The molecule consists of two $(\mu_3\text{-Se})\text{Co}_3$ pyramids, joined by a Se_2 group which bridges one Co–Co edge of each cluster. The $\text{Co}_2\text{Se}_2\text{Co}_2$ array is folded along the diselenide bond (119°), and the two $\mu_3\text{-Se}$ ligands are on the opposite side with respect to the Se–Se hinge. Complex **5** crystallizes in the rhombohedral $R\bar{3}$ space group, with $a = 24.915(4)$ Å, $c = 12.655(3)$ Å, $V = 6803(2)$ Å³, $Z = 9$, and $\rho(\text{calcd}) = 2.877$ Mg/m³. X-ray data were collected using a crystal sealed with mother liquor, and the structure was solved by direct methods and refined (1449 reflections, $F > 4\sigma(F)$) to the final $R = 0.045$ and $wR = 0.053$. The molecule can be described as a Co_6 octahedron, with a centrosymmetric crystallographic symmetry, whose faces are bridged by Se atoms, forming an Se_8 cubic array. One CO group is terminally bonded to each metal atom. A new complex has been isolated from the products of the reaction between $\text{Co}_2(\text{CO})_8$ and CSe_2 in petroleum ether. It has been identified by infrared spectroscopy as $\text{Co}_6(\mu_4\text{-Se})(\mu_6\text{-C}_2)(\text{CO})_{14}$ (**6**), where the six cobalt atoms are arranged in a “boat” configuration and include a semi-interstitial C_2 unit. A $\mu_4\text{-Se}$ atom and 8 terminal and 6 bridging CO groups complete the structure. Infrared and Raman spectra of the complexes are discussed, and the main vibrational modes are assigned and compared with those of the analogous sulfur complexes.

Introduction

The facile reaction of $\text{Co}_2(\text{CO})_8$ with CS_2 at room temperature, first observed by Bor and Markó in the early sixties,¹ gives rise to a plethora of S- and C-containing cobalt carbonyl derivatives. Their structural characterization has shown the CS_2 molecule bonded in unusual manners to cobalt clusters,^{2,3} together with a variety of coordinated ligand-derived fragments, such as CS ,⁴ SCO ,⁵ $\mu_3\text{-C}$,^{2,5} and interstitial $\mu_6\text{-C}$,^{6,7} and C_2 units,⁸ together with S atoms bridging three^{2,3,5} and four^{8–10} cobalt atoms. Some of the same cobalt–sulfur complexes, together with a cuboctahedral $\text{Co}_6\text{S}_8(\text{CO})_6$ cluster,¹¹ were isolated from the reaction of $\text{Co}_2(\text{CO})_8$ with elemental sulfur. These complexes form part of the large family of metal–sulfur compounds

in which the $\mu_3\text{-S}$ and $\mu_4\text{-S}$ ligands stabilize the metal framework with respect to degradation by clamping the metal atoms together.¹²

By comparison, despite the chemical similarity between sulfur and selenium, relatively few examples have been reported involving selenium as a capping ligand. Most have appeared in the last few years and concern clusters of the iron triad;¹³ the only Co–Se cluster, $\text{Co}_3(\mu_3\text{-Se})(\text{CO})_9$ (**1**), was prepared more than 20 years ago by reacting $\text{Co}_2(\text{CO})_8$ and H_2Se at high temperature and CO pressure.¹⁴ The previous experience on $\text{Co}_2(\text{CO})_8/\text{CS}_2/\text{S}_8$ chemistry suggested a study of the reactions of dicobalt octacarbonyl with CSe_2 and with elemental selenium. The synthetic routes were partially described in two papers that appeared last year. They reported the structural characterization and the vibrational properties of two novel cobalt selenium clusters, $\text{Co}_4(\mu_4\text{-Se})_2(\text{CO})_{10}$ (**2**)¹⁰ and $\text{Co}_6(\mu_6\text{-C})(\mu_3\text{-Se})_2(\text{CO})_{12}$ (**3**),¹⁵ both having analogues in the family of Co/S complexes.

[†] Università di Torino.

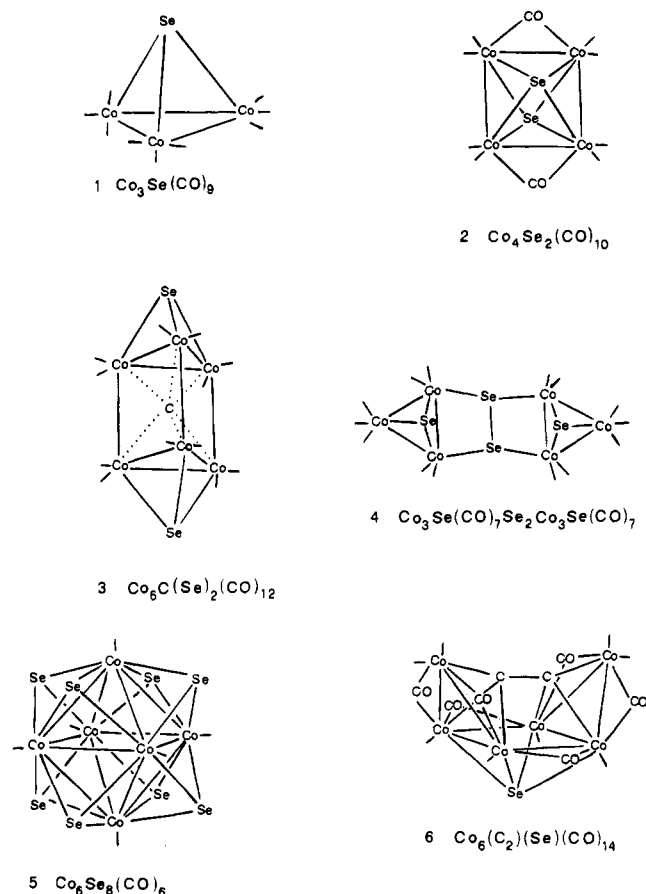
[‡] University of East Anglia and Royal Military College.

[Ⓞ] Abstract published in *Advance ACS Abstracts*, November 15, 1994.

- (1) Markó, L.; Bor, G.; Klumpp, E. *Angew. Chem.* **1963**, *75*, 248.
- (2) Gervasio, G.; Rossetti, R.; Stanghellini, P. L.; Bor, G. *Inorg. Chem.* **1982**, *21*, 3781.
- (3) Wei, C. H. *Inorg. Chem.* **1984**, *23*, 2973.
- (4) Gervasio, G.; Rossetti, R.; Stanghellini, P. L.; Bor, G. *J. Chem. Soc., Dalton Trans.* **1987**, 1707.
- (5) Gervasio, G.; Rossetti, R.; Stanghellini, P. L.; Bor, G. *J. Chem. Soc., Dalton Trans.* **1983**, 1613.
- (6) Bor, G.; Dietler, U. K.; Stanghellini, P. L.; Gervasio, G.; Rossetti, R.; Sbrignadello, G.; Battiston, G. *J. Organomet. Chem.* **1981**, *213*, 277.
- (7) Gervasio, G.; Rossetti, R. *Acta Crystallogr.* **1993**, *C49*, 1262.
- (8) Gervasio, G.; Rossetti, R.; Stanghellini, P. L.; Bor, G. *Inorg. Chem.* **1984**, *23*, 2073.
- (9) Wei, C. H.; Dahl, L. F. *Cryst. Struct. Commun.* **1975**, *4*, 583.
- (10) Gervasio, G.; Rossetti, R.; Stanghellini, P. L.; Braga, D.; Kettle, S. F. A. *J. Cryst. Spectr. Res.* **1993**, *23*, 255.

- (11) Gervasio, G.; Rossetti, R.; Stanghellini, P. L. *Inorg. Chim. Acta* **1984**, *83*, L9–L10. Diana, E.; Gervasio, G.; Rossetti, R.; Valdemarin, F.; Bor, G.; Stanghellini, P. L. *Inorg. Chem.* **1991**, *30*, 294.
- (12) Vahrenkamp, H. In *Studies in Inorganic Chemistry*; Müller, A., Krebs, B., Eds.; Elsevier Publ.: Amsterdam, 1984; Vol. 5, pp 121–139.
- (13) Sappa, E.; Tiripicchio, A.; Braunstein, P. *Coord. Chem. Rev.* **1985**, *65*, 219. Adams, R. D. *Polyhedron* **1985**, *4*, 2003.
- (14) Layer, T. M.; Lewis, J.; Martin, A.; Raithby, P. R.; Wong, W. T. *J. Chem. Soc., Dalton Trans.* **1992**, 3411. Arce, A. J.; Arropo, P.; De Sanctis, Y.; Deeming, A. J.; West, D. J. *Polyhedron* **1992**, *11*, 1013. Johnson, B. F. G.; Layer, T. M.; Lewis, J.; Raithby, P. R.; Wong, W. T. *J. Chem. Soc., Dalton Trans* **1993**, 973. Mathur, P.; Hossain, M. M.; Rashid, R. S. *J. Organomet. Chem.* **1993**, *488*, 211.
- (15) Strouse, C. E.; Dahl, L. F. *J. Am. Chem. Soc.* **1971**, *93*, 6032.

Chart 1



The purpose of the present paper is to complete the survey of the above reactions and at the same time to describe three new selenium complexes, which, again, are homologous to those in the sulfide series. Two, $[(\mu_3\text{-Se})\text{Co}_3(\text{CO})_7]_2\mu_4\text{-(Se}_2)$ (**4**) and $\text{Co}_6(\mu_3\text{-Se})_8(\text{CO})_6$ (**5**), have been characterized by X-ray diffraction, and the third, $\text{Co}_6(\mu_6\text{-C}_2)(\mu_4\text{-Se})(\text{CO})_{14}$ (**6**), has been characterized by spectroscopic methods and comparison with the corresponding sulfide cluster (Chart 1).

Experimental Section

All experimental procedures were carried out by Schlenk techniques under a nitrogen or CO atmosphere in a N_2 -filled vacuum glovebox equipped with a recirculating system. Reagent grade solvents were distilled and stored under nitrogen after drying by standard methods. $\text{Co}_2(\text{CO})_8$ and CSe_2 were purchased from Strem Chemical and Alfa, respectively, and used as received. The commercially available black selenium is unreactive; the reactive form is the amorphous red selenium formed by precipitation from aqueous solutions of selenious acid by treatment with SO_2 . The crude product was extracted by CS_2 in a Soxhlet apparatus; preparation details have been given elsewhere.¹⁶ Particular care should be used to remove traces of CS_2 from the final product, owing to the reactivity of carbon disulfide with dicobalt octacarbonyl.

Spectroscopic Measurement. Infrared spectra were recorded on Perkin-Elmer PE580 and Bruker IFS113-FTIR instruments at $1\text{--}2\text{ cm}^{-1}$ resolution. Samples were measured in pressed KBr disks ($4000\text{--}300\text{ cm}^{-1}$), in *n*-heptane solutions ($2200\text{--}1700\text{ cm}^{-1}$) and in polyethylene disks ($400\text{--}50\text{ cm}^{-1}$). Raman spectra were recorded on polycrystalline samples with a Bruker IFS 66 FTIR spectrometer together with an FRA

106 FT-Raman module; the incident YAG laser power was 80 mW and the resolution 4 cm^{-1} .

Reactions. Owing to the complexity of the reactions between $\text{Co}_2(\text{CO})_8$ and CSe_2 or Se, we have simply reported in previous papers descriptions concerned largely with the isolation of complexes **2**¹⁰ and **3**¹⁵. The detailed chemical manipulations are described below.

Reaction of $\text{Co}_2(\text{CO})_8$ with CSe_2 . A solution of $\text{Co}_2(\text{CO})_8$ (5 g, 14.5 mmol in 500 mL of petroleum ether) was cooled at 0°C under a continuous flux of nitrogen. A ca. 2 mL volume of CSe_2 was syringed drop by drop into the reaction mixture maintaining vigorous stirring. The reaction was monitored by checking the typical infrared $\nu(\text{CO})$ absorption of $\text{Co}_2(\text{CO})_8$. The reaction is very fast: $\text{Co}_2(\text{CO})_8$ disappears in less than 10 min. Owing to the possible polymerization of CSe_2 , part of the starting $\text{Co}_2(\text{CO})_8$ does not react and the subsequent addition of few drops of CSe_2 is usually necessary to complete the reaction. The mixture was allowed to warm to room temperature and filtered. The residue was repeatedly extracted with small aliquots of THF, until the solution appeared colorless. The brown solution was concentrated to ca. 100 mL and stored at -20°C : complex **2** was obtained as black microcrystals (yield ca. 0.9 g).

The reaction solution was concentrated to ca. 100 mL, and it was chromatographed on a column (diameter 4 cm, height 40 cm) prepared with 120 g of silica gel 60 (70–230 mesh; Merck). Elution with petroleum ether developed four bands, whose colors were, in order, pink-brown, green, dark-brown, and red-brown. The elutes were separately collected, concentrated, and allowed to crystallize. The first three compounds were subsequently identified as **1** (yield ca. 1 g), **3** (yield ca. 0.8 g), and $\text{Co}_4(\text{CO})_{12}$ (yield ca. 0.5 g). Complex **1** must be collected and stored under CO to avoid decomposition. The fourth red brown band (apparent yield less than 1%) corresponds to a carbonyl complex ($\nu(\text{CO})$ at 2083 (s), 2060 (s), 2045 (m), and 2039 (m) cm^{-1} in petroleum ether), so unstable as to prevent any attempt at identification. Subsequent elution with CHCl_3 developed another olive green band, whose similar treatment gave rise to **6** (yield ca. 0.04 g).

Reaction of $\text{Co}_2(\text{CO})_8$ with Red Selenium. The main products of this reaction are complexes **2**, **4**, and **5**. Different reaction conditions and subsequent chemical manipulations can vary the relative yield of the products. We now describe two typical procedures, leading to the maximum yields of complexes **4** and **5**, respectively.

(a) Under a CO atmosphere 5 g (14.5 mmol) of $\text{Co}_2(\text{CO})_8$ and 1.15 g (14.5 mmol) of red selenium in 500 mL of THF were stirred at room temperature. After 24 h the $\text{Co}_2(\text{CO})_8$ completely disappeared, shown by infrared spectroscopy. The mixture was filtered and the residue worked up as reported in the previous reaction: final crystallization gave 1.3 g of complex **2**. The solid obtained from the filtered solution after removal of residual solvent in vacuum was chromatographed on a florisil column (100–200 mesh Merck). Elution with petroleum ether gave, first, a trace amount of complex **2**, followed by a large violet band, which was collected, concentrated to ca. 100 mL, and allowed to crystallize at -20°C . Microcrystals of complex **4**, suitable for X-ray diffraction, were obtained (yield 3.2 g).

(b) A suspension of 4.6 g of selenium (58.2 mmol) in 300 mL of THF was stirred for several minutes under a gentle flux of carbon monoxide at room temperature. A solution of 4 g of $\text{Co}_2(\text{CO})_8$ (11.7 mmol) in 150 mL of THF was added dropwise by means of a percolating funnel. The mixture was stirred and fluxed until $\text{Co}_2(\text{CO})_8$ disappeared (ca. 24 h). The solvent was removed in vacuum, and the residue was extracted with 20 mL aliquots of petroleum ether, until the solvent was colorless. The resulting violet solution contained almost pure complex **4**; if necessary, it was chromatographed and/or crystallized, as reported before (yield ca. 2.2 g). The residue contained, *inter alia*, complex **2** and complex **5**, whose solubility in CCl_4 is $5 \gg 2$. So, repeated extraction with 10 mL aliquots of CCl_4 , until the green color disappeared, allowed complex **5** to be obtained. This was purified by chromatography on a florisil column (eluant CCl_4). Removal of the eluant gave 300 mg of complex **5**. A subsequent, more extended, workup of the residue with larger aliquots of CHCl_3 at ca. 40°C yielded ca. 0.8 g of complex **2**.

Crystal Structure Analysis. The crystals of complex **4** were of poor quality but stable in air, and it was possible to carry out a structure determination. The crystallographic data are shown in Table 1. The

(15) Gervasio, G.; Rossetti, R.; Stanghellini, P. L.; Kettle, S. F. A.; Bor, G. *Spectrochim. Acta* **1993**, *49A*, 1401.

(16) Ginsberg, A. P.; Osborne, J. H.; Sprinkle, B. R. *Inorg. Chem.* **1983**, *22*, 12.

Table 1. Crystal Data for $[\text{Co}_3\text{Se}(\text{CO})_7]_2\text{Se}_2$ (Complex **4**) and $[\text{Co}_6\text{Se}_8(\text{CO})_6]_2\text{C}_6\text{H}_6$ (Complex **5**)

	4	5
formula	$\text{C}_{14}\text{Co}_6\text{O}_{14}\text{Se}_4$	$\text{C}_{18}\text{H}_{12}\text{Co}_6\text{O}_6\text{Se}_8$
fw	1061.6	1319.5
space group	$P\bar{1}$	$R\bar{3}$
a , Å	9.649(2)	24.915(4)
b , Å	12.688(3)	
c , Å	12.952(6)	12.655(3)
α , deg	66.61(3)	
β , deg	71.89(3)	
γ , deg	83.53(2)	
V , Å ³	1383.1(8)	6803(2)
Z	2	9
ρ_{calcd} , g cm ⁻³	2.549	2.877
μ , cm ⁻¹	88.37	119.22
T , °C	20	20
transm coeff	0.990–0.349	0.009–0.001
R^a (obsd data)	0.0808	0.0445
wR^b (obsd data)	0.1068	0.0534

$$^a R = \sum(|F_o - F_c|) / \sum F_o, \quad ^b wR = [\sum w(|F_o - F_c|)^2 / \sum (wF_o)^2]^{1/2}.$$

Table 2. Atomic Coordinates ($\times 10^4$) and Equivalent Isotropic Displacement Coefficients ($\text{Å}^2 \times 10^3$) for $[\text{Co}_3\text{Se}(\text{CO})_7]_2\text{Se}_2$

	x	y	z	$U(\text{eq})^a$
Co(1)	3264(4)	2872(3)	6365(3)	46(2)
Co(2)	1211(4)	1461(3)	7109(3)	45(2)
Co(3)	3507(4)	820(3)	7796(3)	53(2)
Co(4)	2633(4)	4244(3)	3130(3)	44(2)
Co(5)	610(4)	2785(3)	3832(3)	43(2)
Co(6)	1838(4)	3822(3)	1622(3)	44(2)
Se(1)	1933(3)	4177(2)	5094(3)	45(2)
Se(2)	43(3)	2837(2)	5746(3)	47(2)
Se(3)	3445(3)	1289(2)	5911(3)	56(2)
Se(4)	401(3)	4706(2)	2815(3)	49(2)
C(11)	5065(34)	3466(24)	5538(27)	56(8)
O(11)	6155(29)	3771(21)	4998(23)	100(8)
C(12)	2834(37)	3473(28)	7399(30)	69(9)
O(12)	2524(26)	3846(20)	8130(22)	90(7)
C(21)	267(34)	191(27)	7319(27)	63(9)
O(21)	-240(25)	-659(20)	7493(20)	83(7)
C(22)	119(33)	1780(25)	8283(27)	58(9)
O(22)	-629(30)	2018(23)	9089(25)	113(9)
C(31)	5400(45)	917(32)	7551(33)	91(12)
O(31)	6653(32)	1041(22)	7399(23)	106(9)
C(32)	3175(34)	-714(27)	8325(28)	64(9)
O(32)	2887(26)	-1656(21)	8632(21)	91(7)
C(33)	2749(43)	996(32)	9115(36)	92(12)
O(33)	2264(33)	1170(25)	9978(30)	133(11)
C(41)	3515(36)	5638(29)	2336(29)	71(10)
O(41)	3988(32)	6523(26)	1896(26)	119(9)
C(42)	4156(33)	3363(24)	3123(25)	53(8)
O(42)	5198(24)	2790(18)	3059(19)	77(7)
C(51)	-1116(40)	2259(28)	3986(29)	74(10)
O(51)	-2204(29)	1934(21)	3998(21)	92(7)
C(52)	1543(33)	1474(25)	3990(25)	56(8)
O(52)	2120(24)	606(19)	4154(20)	83(7)
C(61)	510(36)	3532(25)	1041(28)	62(9)
O(61)	-369(28)	3411(20)	663(22)	93(8)
C(62)	2897(40)	4978(32)	391(34)	86(11)
O(62)	3577(28)	5693(22)	-335(24)	101(8)
C(63)	3034(31)	2650(24)	1522(24)	51(8)
O(63)	3845(27)	1943(21)	1415(22)	90(7)

^a Equivalent isotropic U defined as one-third of the trace of the orthogonalized U_{ij} tensor.

fractional atomic coordinates and the equivalent isotropic displacement coefficients are detailed in Table 2.

The solid obtained by evaporating or cooling solutions of complex **5** was always a finely divided powder, not suitable for X-ray analysis. Crystals of adequate dimensions were grown by the following method. A beaker half filled with a saturated solution of **5** in benzene was immersed in a bath of *n*-hexane. The apparatus was deaerated with a gentle flux of nitrogen and then carefully closed and left to stand for

Table 3. Atomic Coordinates ($\times 10^4$) and Equivalent Isotropic Displacement Coefficients ($\text{Å}^2 \times 10^3$) for $[\text{Co}_6\text{Se}_8(\text{CO})_6]_2\text{C}_6\text{H}_6$

	x	y	z	$U(\text{eq})^a$
Se(1)	2617(1)	557(1)	5535(1)	67(1)
Se(2)	3011(1)	1933(1)	4680(1)	69(1)
Se(3)	4412(1)	2446(1)	5503(1)	69(1)
Se(4)	4034(1)	1070(1)	6373(1)	66(1)
Co(1)	3568(1)	1456(1)	5232(1)	62(1)
Co(2)	4222(1)	1990(1)	7186(1)	64(1)
Co(3)	3091(1)	796(1)	7204(1)	62(1)
C(11)	3750(7)	1253(7)	4030(12)	78(8)
O(11)	3873(6)	1114(6)	3257(9)	113(7)
C(21)	4952(8)	2239(7)	7580(12)	80(9)
O(21)	5457(6)	2420(5)	7863(11)	116(7)
C(31)	2901(6)	60(7)	7592(12)	73(7)
O(31)	2782(5)	-425(5)	7835(9)	100(6)
C(1)	5880(9)	1591(9)	5848(18)	123(6)
C(2)	5472(9)	1115(10)	5185(16)	120(6)
C(3)	5243(8)	1226(9)	4298(15)	108(5)
C(4)	5409(8)	1811(8)	4065(15)	106(5)
C(5)	5808(8)	2259(9)	4701(14)	110(5)
C(6)	6041(10)	2158(10)	5605(16)	121(6)

^a Equivalent isotropic U defined as one-third of the trace of the orthogonalized U_{ij} tensor.

at least 2 weeks at room temperature. The slow migration of *n*-hexane into the benzene solution led to slowly grown crystals, whose formula was established as $[\text{Co}_6\text{Se}_8(\text{CO})_6]_2\text{C}_6\text{H}_6$ by the resolution of the structure. The crystals, when separated from the solution, rapidly lost the lattice benzene molecules, even if they retained the external shape. A crystal suitable for X-ray analysis was therefore rapidly removed from the solution and sealed with mother liquor into a Lindemann glass capillary. No deterioration was observed during the crystallographic measurements. The crystallographic data are listed in Table 1; the atomic fractional coordinates and the equivalent isotropic displacement coefficients are listed in Table 3. The hydrogen atoms were put in calculated positions and refined riding on the corresponding carbon atoms with a constant isotropic temperature factor.

The diffraction data were collected on a Nicolet R3 (complex **4**) and on a Siemens P4 (complex **5**) diffractometers in the α scan mode with Mo $K\alpha$ radiation ($\lambda = 0.71073$) and a graphite monochromator. A total of 2302 (complex **4**) and 10 266 (complex **5**) reflections were collected, and only those with $F > 4.0 \sigma(F)$ were considered observed, after merging the equivalent ones.

The Co and Se atoms were located by direct methods, and the C and O atoms, by subsequent Fourier-difference maps. The softwares used for solution and refinement were SHELX76 (complex **4**) and SHELXTL PLUS, PC version (complex **5**).

For both compounds an absorption correction was applied by the method described in ref 17.

Full list of the parameters utilized in the intensity collection and refinement together with the crystallographic data are presented in the supplementary material.

Results and Discussion

Complex 4. Description of the Structure. The molecule is formed by two pyramidal Co_3Se clusters in which the Co–Co edges of each are parallel. The two edges are then bridged by a Se_2 group, so there are two Co–Se–Co bridges in the molecule (Figure 1). The $\text{Se}_{\text{eq}}\text{--Se}_{\text{eq}}$ bond is nearly coplanar with the Co_3 plane in each metal triangle and the two Co_3Se_2 planes form a dihedral angle of 119° . Relevant distances and angles are listed in Table 4.

A similar complex was obtained with sulfur.¹⁸ Considering the rather rigid arrangement around the E–E bond (E = S, Se), in principle three isomers could be obtained, as shown in Chart

(17) North, A. C. T.; Phillips, D. C.; Mathews, F. S. *Acta Crystallogr.* **1968**, A24, 351.

(18) Stevenson, D. L.; Magnuson, V. R.; Dahl, L. F. *J. Am. Chem. Soc.* **1967**, 89, 3727.

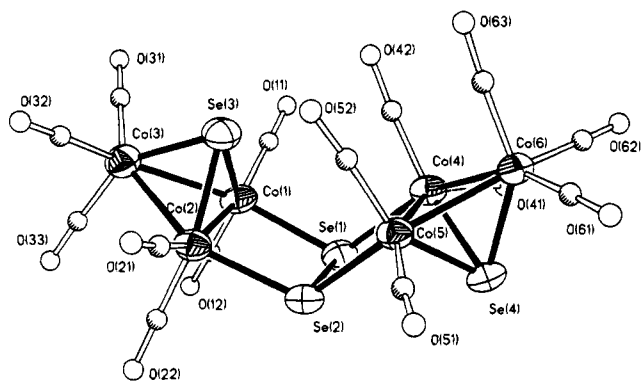


Figure 1. ORTEP plot (50% of probability) of complex **4** with the atom-labeling scheme.

2. In two isomers (a and b) the apical chalcogen atoms are on the same side of the bridge; in the third isomer (c), they are in an anti configuration.

The sulfur compound was obtained in the (a) form only, and the selenium complex in the (c) form only. The absence of isomer (b) in both cases and the absence of isomer (a) for selenium compound is probably to be associated with the greater steric hindrance of axial CO groups near the bridge and by the steric hindrance between the $\text{Se}_{\text{ap}} \cdots \text{Se}_{\text{ap}}$ atoms, respectively. In order to evaluate the steric hindrances of the isomers, their ideal geometries were built on by using the program Moldraw¹⁹ and the intermolecular contacts were calculated. The resulting $\text{Se}_{\text{ap}} \cdots \text{Se}_{\text{ap}}$ distance was 3.19 Å, not so great as to exclude completely the existence of isomer (a), while the distance between the oxygen atoms of the eclipsed axial CO's seems to render the isomer (b) unstable for both chalcogen derivatives: e.g., the calculated O \cdots O distance was nearly 2.0 Å for the (b) isomer, when E = Se.

Inspection of the Co_3Se clusters shows the expected enlargement from the S to the Se species together with an asymmetry in the Co_3 triangle. For instance, the Co–Co bonds bridged by the $\text{Se}_{\text{eq}}-\text{Se}_{\text{eq}}$ are shorter (6–10 σ) than the other two. There are two different Co–Se distances in this complex, Co– Se_{ap} and Co– Se_{eq} . The latter has an average value of 2.397(6) Å while the former is shorter (2.286(6) Å average). This pattern has already been observed in analogous sulfur compounds, for which a large amount of data exist.^{2,4,18,20,21} The Se(1)–Se(2) bond distance (2.352(4)Å) corresponds to the distance found in the Se_8 molecule (2.33Å) and in metallic Se (2.37Å).²² The Co– Se_{ap} value lies in the lower part of the range found for $\text{Co}_3(\mu_3\text{-Se})$ units. The following Co–Se values (Å) are known: 2.282 in $\text{Co}_3\text{Se}(\text{CO})_9$;¹⁴ 2.33–2.37²³ and 2.322–2.373²⁴ in $\text{Co}_6\text{Se}_8(\text{PPh}_3)_6$, corresponding to crystal packing with the inclusion of different solvent molecules; 2.337–2.375 in $\text{Co}_4\text{Se}_4(\text{PPh}_3)_4$;²³ 2.28–2.36 in $\text{Co}_9\text{Se}_{11}(\text{PPh}_3)_6$;²³ 2.32–2.40 in $[\text{Co}_6\text{Se}_8(\text{PPh}_3)_6]^{+}$;²⁵ 2.239–2.418 in $[\text{Co}_8\text{Se}_8(\text{PPh}_3)_6]^{+}$;²⁵ 2.281–2.446 in $\text{Co}_6\text{Se}_8(\text{PPh}_3)_6$;²⁵ and 2.319 (average) in $\text{Co}_6\text{CSe}_2(\text{CO})_{12}$.¹⁵ Each Co atom links two equatorial groups (CO or

Table 4. Relevant Bond Lengths (Å) and Angles (deg) for $[\text{Co}_3\text{Se}(\text{CO})_7]_2\text{Se}_2$

Co(1)–Co(2)	2.510(6)	Co(1)–Co(3)	2.563(5)
Co(1)–Se(1)	2.402(5)	Co(1)–Se(3)	2.282(6)
Co(1)–C(11)	1.798(29)	Co(1)–C(12)	1.715(42)
Co(2)–Co(3)	2.570(6)	Co(2)–Se(2)	2.404(5)
Co(2)–Se(3)	2.277(5)	Co(2)–C(21)	1.824(37)
Co(2)–C(22)	1.728(33)	Co(3)–Se(3)	2.290(6)
Co(3)–C(31)	1.763(44)	Co(3)–C(32)	1.818(33)
Co(3)–C(33)	1.730(46)	Co(4)–Co(5)	2.537(6)
Co(4)–Co(6)	2.559(7)	Co(4)–Se(1)	2.389(6)
Co(4)–Se(4)	2.285(5)	Co(4)–C(41)	1.805(33)
Co(4)–C(42)	1.744(30)	Co(5)–Co(6)	2.566(5)
Co(5)–Se(2)	2.393(6)	Co(5)–Se(4)	2.285(4)
Co(5)–C(51)	1.788(42)	Co(5)–C(52)	1.769(30)
Co(6)–Se(4)	2.295(5)	Co(6)–C(61)	1.808(42)
Co(6)–C(62)	1.790(31)	Co(6)–C(63)	1.798(29)
Se(1)–Se(2)	2.352(4)	C(11)–O(11)	1.079(37)
C(12)–O(12)	1.165(52)	C(21)–O(21)	1.145(45)
C(22)–O(22)	1.198(45)	C(31)–O(31)	1.181(55)
C(32)–O(32)	1.137(43)	C(33)–O(33)	1.168(61)
C(41)–O(41)	1.114(45)	C(42)–O(42)	1.174(37)
C(51)–O(51)	1.164(52)	C(52)–O(52)	1.148(37)
C(61)–O(61)	1.153(53)	C(62)–O(62)	1.100(39)
C(63)–O(63)	1.144(39)		
Co(2)–Co(1)–Co(3)	60.9(2)	Co(2)–Co(1)–Se(1)	87.0(2)
Co(3)–Co(1)–C(11)	108.3(9)	Se(1)–Co(1)–C(11)	98.8(10)
Co(2)–Co(1)–C(12)	102.7(11)	Co(3)–Co(1)–C(12)	95.6(10)
Se(1)–Co(1)–C(12)	97.4(11)	C(11)–Co(1)–C(12)	99.9(17)
Co(1)–Co(2)–Co(3)	60.6(2)	Co(1)–Co(2)–Se(2)	89.2(2)
Co(3)–Co(2)–C(21)	108.7(10)	Se(2)–Co(2)–C(21)	96.8(11)
Co(1)–Co(2)–C(22)	100.2(11)	Co(3)–Co(2)–C(22)	99.1(12)
Se(2)–Co(2)–C(22)	93.2(10)	C(21)–Co(2)–C(22)	100.6(15)
Co(1)–Co(3)–Co(2)	58.5(2)	Co(1)–Co(3)–C(31)	95.5(11)
Co(2)–Co(3)–C(32)	96.1(12)	C(31)–Co(3)–C(32)	103.5(16)
Co(1)–Co(3)–C(33)	99.5(12)	Co(2)–Co(3)–C(33)	94.4(15)
C(31)–Co(3)–C(33)	103.6(22)	C(32)–Co(3)–C(33)	98.5(16)
Co(5)–Co(4)–Co(6)	60.4(2)	Co(5)–Co(4)–Se(1)	87.1(2)
Co(6)–Co(4)–C(41)	105.3(14)	Se(1)–Co(4)–C(41)	100.3(13)
Co(5)–Co(4)–C(42)	101.0(11)	Co(6)–Co(4)–C(42)	96.7(13)
Se(1)–Co(4)–C(42)	101.3(11)	C(41)–Co(4)–C(42)	100.1(14)
Co(4)–Co(5)–Co(6)	60.2(2)	Co(4)–Co(5)–Se(2)	88.5(2)
Se(2)–Co(5)–Se(4)	97.5(2)	Co(6)–Co(5)–C(51)	107.0(11)
Se(2)–Co(5)–C(51)	97.8(12)	Co(4)–Co(5)–C(52)	103.7(10)
Co(6)–Co(5)–C(52)	96.6(9)	Se(2)–Co(5)–C(52)	103.1(11)
C(51)–Co(5)–C(52)	96.2(16)	Co(4)–Co(6)–Co(5)	99.4(2)
Co(5)–Co(6)–C(61)	99.9(9)	Co(4)–Co(6)–C(62)	94.0(17)
C(61)–Co(6)–C(62)	102.7(18)	Co(5)–Co(6)–C(63)	93.8(8)
Se(4)–Co(6)–C(63)	146.8(10)	C(61)–Co(6)–C(63)	97.5(16)
C(62)–Co(6)–C(63)	99.4(15)	Co(1)–Se(1)–Co(4)	116.0(2)
Co(1)–Se(1)–Se(2)	93.1(1)	Co(4)–Se(1)–Se(2)	93.1(2)
Co(2)–Se(2)–Co(5)	117.5(2)	Co(2)–Se(2)–Se(1)	90.7(2)
Co(5)–Se(2)–Se(1)	91.4(1)	Co(1)–Se(3)–Co(2)	66.8(2)
Co(1)–Se(3)–Co(3)	68.2(2)	Co(2)–Se(3)–Co(3)	68.5(2)
Co(4)–Se(4)–Co(5)	67.5(2)	Co(4)–Se(4)–Co(6)	67.9(2)
Co(5)–Se(4)–Co(6)	68.1(2)	Co(1)–C(11)–O(11)	174.8(34)
Co(1)–C(12)–O(12)	177.7(27)	Co(2)–C(21)–O(21)	174.3(32)
Co(2)–C(22)–O(22)	179.0(32)	Co(3)–C(31)–O(31)	176.0(43)
Co(3)–C(32)–O(32)	175.5(29)	Co(3)–C(33)–O(33)	176.7(38)
Co(4)–C(41)–O(41)	175.3(34)	Co(4)–C(42)–O(42)	176.7(23)
Co(5)–C(51)–O(51)	174.9(31)	Co(5)–C(52)–O(52)	176.4(29)
Co(6)–C(61)–O(61)	176.0(29)	Co(6)–C(62)–O(62)	177.0(50)
Co(6)–C(63)–O(63)	176.6(23)		

Se) and one axial (CO) ligand with angles around the cobalt atoms which are in the normal range.

The $\text{Se} \cdots \text{Se}$ and the $\text{Se} \cdots \text{O}$ intermolecular contacts are shorter than the sum of the Van der Waals radii: e.g. the $\text{Se}(1) \cdots \text{Se}(4)$ contact is 3.598 Å and the $\text{Se}(1) \cdots \text{O}(11)$ contact is 3.300 Å.

Vibrational Analysis. Figure 2 illustrates the $\nu(\text{CO})$ spectra of **4**, together with that of the corresponding sulfur compound. The close similarity between the two patterns clearly indicates that the overall molecular symmetry is not dominant because the predictions are different for the S complex (C_{2v} symmetry)

- (19) Ugliengo, P.; Viterbo, D.; Chiari, G. *Z. Kristallogr.* **1993**, *207*, 9.
 (20) Benoit, A.; Darchen, A.; Le Marouille, J. Y.; Mahe, C.; Patin, H. *Organometallics* **1983**, *2*, 555.
 (21) Markó, L.; Gervasio, G.; Stanghellini, P. L.; Bor, G. *Transition Met. Chem.* **1985**, *10*, 344.
 (22) Wells, A. F. *Structural Inorganic Chemistry*; Clarendon Press: Oxford, U.K., 1984.
 (23) Fenske, D.; Ohmer, J.; Hachgenei, J. *Angew. Chem., Int. Ed. Engl.* **1985**, *24*, 993.
 (24) Hong, M.; Huang, Z.; Lei, X.; Wei, G.; Kang, B.; Liu, H. *Polyhedron* **1991**, *10*, 927.
 (25) Fenske, D.; Ohmer, J.; Merzweiler, K. *Z. Naturforsch.* **1987**, *42B*, 803.

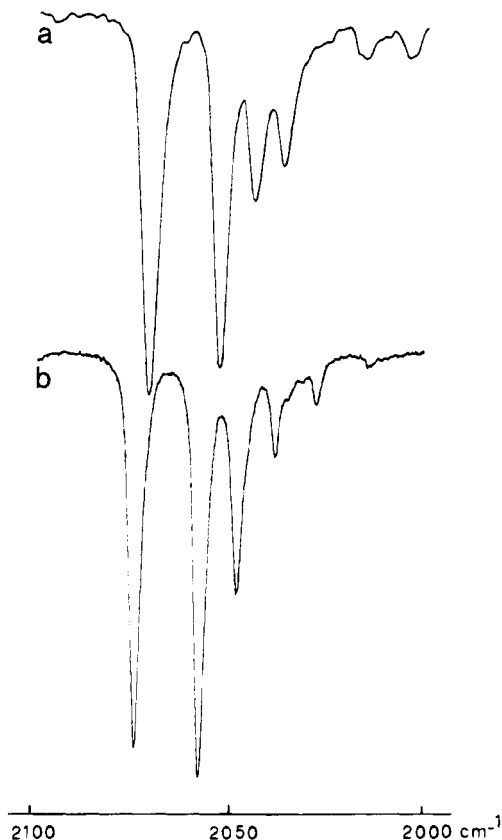
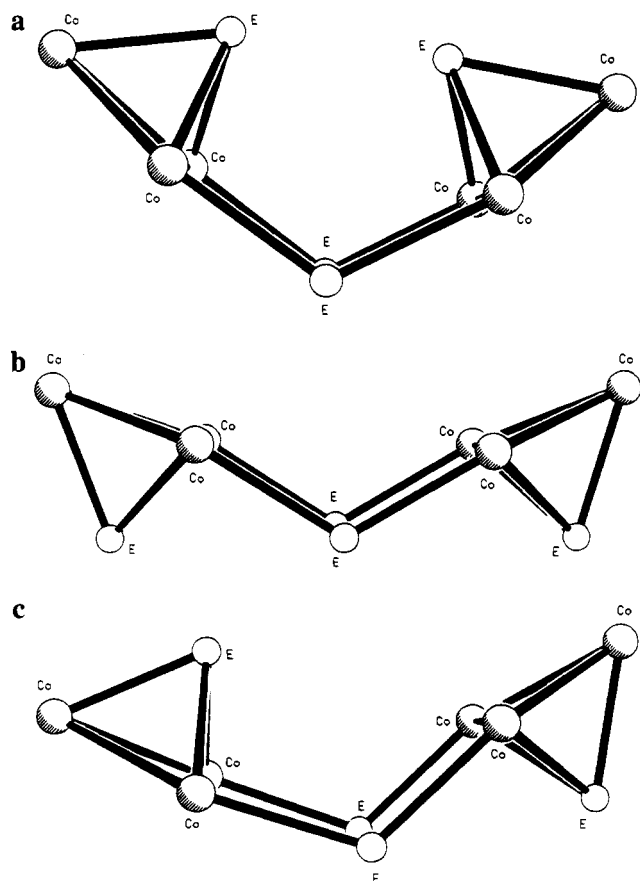


Figure 2. Infrared spectra (*n*-heptane solution) of the $[(\mu_3\text{-E})\text{Co}_3(\text{CO})_7]_2\mu_4\text{-}(\text{E}_2)$ complexes: (a) E = Se (complex 4); (b) E = S.

Chart 2



from the Se complex (C_S symmetry). The actual spectrum corresponds to what is expected for the $\text{Co}_3(\mu_3\text{-E})(\text{CO})_7(\text{E}_2)$ unit

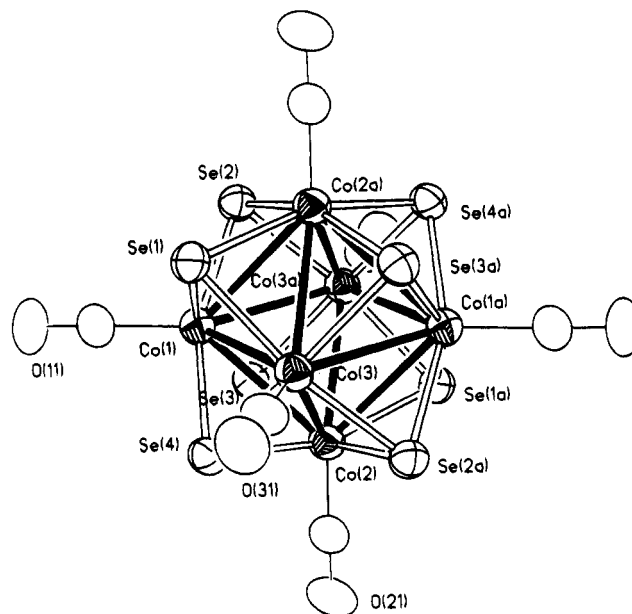


Figure 3. ORTEP plot (30% of probability) of complex 5 with the atom-labeling scheme. Letter "a" refers to atoms related by the inversion center in the middle of the molecule.

(local symmetry C_S , 7 \sim IR active modes allowed): any coupling between the two units is not spectrally evident and may be ignored.

It is interesting that a complex with similar molecular unit²¹ shows only five bands (one of which is weak) in this spectral region. The origin of this difference is not immediately evident and already merits further studies.

Complex 5. Description of the Structure. The complex is formed by a Co_6 octahedron (Figure 3) with each metal atom linked to a terminal CO group; each Co_3 face of the octahedron is capped by an Se atom. The complex is the homologue of the corresponding sulfur complex.¹¹ The molecule lies on a crystallographic inversion center, while the C_6H_6 molecule is in a general position. Relevant bond distances and angles are listed in Table 5. The complex belongs to the well-known class with formula $[\text{Co}_6\text{Se}_8\text{L}_6]$.^{22,23,24} The Co–Se distances (2.342–(2) Å average) are in keeping with other complexes containing Co_3Se moieties and lie in the range previously reported (see above). The Co–Co distances, 2.892–2.916 Å, differ slightly from those of the three other known $\text{Co}_6\text{Se}_8\text{L}_6$ clusters (Å): 2.99–3.02 for $\text{Co}_6\text{Se}_8(\text{PPh}_3)_6\text{C}_2\text{H}_4\text{Cl}_2$;²³ 2.955–3.037 for $\text{Co}_6\text{Se}_8(\text{PPh}_3)_6\text{THF}$;²⁴ 2.86–2.93 for $[\text{Co}_6\text{Se}_8\text{PPh}_3]_6^+$.²⁵ In fact, they are smaller than those of the analogous PPh_3 neutral derivatives and better resemble those of the monocationic species. A parallel behavior occurs in the corresponding $\text{Co}_6\text{S}_8(\text{CO})_6$, $\text{Co}_6\text{S}_8(\text{PPh}_3)_6$, and $[\text{Co}_6\text{S}_8(\text{PPh}_3)_6]^+$ series. The complex could also be represented as an Se_8 cube with edges spanning from 3.245 to 3.273 Å, inscribing a Co_6 octahedron with the cobalt atoms protruding 0.42 Å out of the Se_4 faces.

As in complex 4, the $\text{Se}\cdots\text{Se}$ intermolecular contacts are shorter than the sum of Van der Waals radii: the values are 3.553 and 3.746 Å, with Se(1) contacting two Se atoms (Se(2) and Se(4)) of adjacent molecules around the 3-fold screw axis.

Vibrational Analysis. The idealized molecular structure of 5 belongs to the O_h group, as does the isostructural $\text{Co}_6\text{S}_8(\text{CO})_6$. All the data concerning the distribution of the normal modes of vibration among the symmetry species, the approximate description of these modes, and their IR or Raman activity have been previously detailed,¹¹ a discussion germane to the comparison of the features of the S/Se spectra.

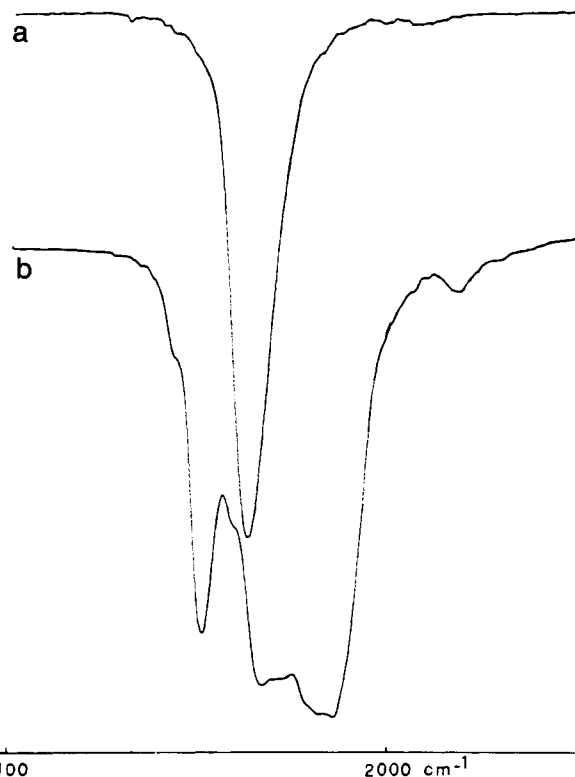
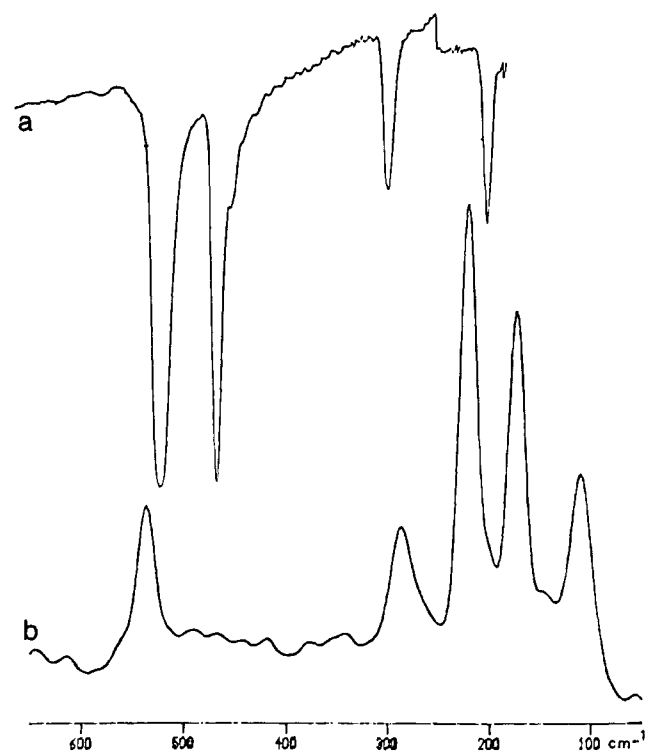
Table 5. Relevant Bond Lengths (Å) and Angles (deg) for $[\text{Co}_6\text{Se}_8(\text{CO})_6]_e \cdot 2\text{C}_6\text{H}_6$

Se(1)—Co(1)	2.340(2)	Se(1)—Co(3)	2.347(2)
Se(1)—Co(2a)	2.339(3)	Se(2)—Co(1)	2.342(3)
Se(2)—Co(2a)	2.350(2)	Se(2)—Co(3a)	2.343(2)
Se(3)—Co(1)	2.332(2)	Se(3)—Co(2)	2.349(2)
Se(3)—Co(3a)	2.345(3)	Se(4)—Co(1)	2.339(3)
Se(4)—Co(2)	2.336(3)	Se(4)—Co(3)	2.342(2)
Co(1)—Co(2)	2.892(2)	Co(1)—Co(3)	2.895(2)
Co(1)—C(11)	1.733(17)	Co(1)—Co(2a)	2.911(3)
Co(1)—Co(3a)	2.916(3)	Co(2)—Co(3)	2.898(2)
Co(2)—C(21)	1.678(18)	Co(2)—Co(3a)	2.905(3)
Co(3)—C(31)	1.721(17)	C(11)—O(11)	1.129(21)
C(21)—O(21)	1.160(22)	C(31)—O(31)	1.134(21)
Co(1)—Se(1)—Co(3)	76.3(1)	Co(1)—Se(1)—Co(2a)	76.9(1)
Co(3)—Se(1)—Co(2a)	76.6(1)	Co(1)—Se(2)—Co(2a)	76.7(1)
Co(1)—Se(2)—Co(3a)	77.0(1)	Co(2a)—Se(2)—Co(3a)	76.3(1)
Co(1)—Se(3)—Co(2)	76.3(1)	Co(1)—Se(3)—Co(3a)	77.1(1)
Co(2)—Se(3)—Co(3a)	76.5(1)	Co(1)—Se(4)—Co(2)	76.4(1)
Co(1)—Se(4)—Co(3)	76.4(1)	Co(2)—Se(4)—Co(3)	76.6(1)
Se(1)—Co(1)—Se(2)	87.8(1)	Se(2)—Co(1)—Se(3)	87.5(1)
Se(1)—Co(1)—Se(4)	88.8(1)	Se(3)—Co(1)—Se(4)	88.5(1)
Co(2)—Co(1)—Co(3)	60.1(1)	Se(1)—Co(1)—C(11)	98.7(4)
Se(2)—Co(1)—C(11)	101.2(7)	Se(3)—Co(1)—C(11)	102.0(4)
Se(4)—Co(1)—C(11)	99.6(7)	Co(2)—Co(1)—Co(2a)	89.8(1)
Co(3)—Co(1)—Co(2a)	60.0(1)	Co(2)—Co(1)—Co(3a)	60.0(1)
Co(3)—Co(1)—Co(3a)	90.0(1)	Co(2a)—Co(1)—Co(3a)	59.7(1)
Se(3)—Co(2)—Se(4)	88.2(1)	Co(1)—Co(2)—Co(3)	60.0(1)
Se(3)—Co(2)—C(21)	99.8(5)	Se(4)—Co(2)—C(21)	98.2(7)
Se(3)—Co(2)—Se(1a)	88.4(1)	C(21)—Co(2)—Se(1a)	102.1(7)
Se(4)—Co(2)—Se(2a)	88.4(1)	C(21)—Co(2)—Se(2a)	101.4(5)
Se(1a)—Co(2)—Se(2a)	87.6(1)	Co(1)—Co(2)—Co(1a)	90.2(1)
Co(3)—Co(2)—Co(1a)	60.3(1)	Co(1)—Co(2)—Co(3a)	60.4(1)
Co(3)—Co(2)—Co(3a)	90.2(1)	Co(1a)—Co(2)—Co(3a)	59.7(1)
Se(1)—Co(3)—Se(4)	88.5(1)	Co(1)—Co(3)—Co(2)	59.9(1)
Se(1)—Co(3)—C(31)	98.7(5)	Se(4)—Co(3)—C(31)	98.1(5)
Se(4)—Co(3)—Se(2a)	88.4(1)	C(31)—Co(3)—Se(2a)	102.6(5)
Se(1)—Co(3)—Se(3a)	88.3(1)	C(31)—Co(3)—Se(3a)	102.8(5)
Se(2a)—Co(3)—Se(3a)	87.1(1)	Co(1)—Co(3)—Co(1a)	90.0(1)
Co(2)—Co(3)—Co(1a)	60.1(1)	Co(1)—Co(3)—Co(2a)	60.2(1)
Co(2)—Co(3)—Co(2a)	89.8(1)	Co(1a)—Co(3)—Co(2a)	59.6(1)
Co(1)—C(11)—O(11)	178.7(17)	Co(2)—C(21)—O(21)	178.8(19)
Co(3)—C(31)—O(31)	178.7(14)		

The unique IR active CO stretching mode (T_{1u}) appears as strong band at 2036 cm^{-1} (Figure 4). The higher frequency of the absorption of the S analogue (2058 cm^{-1}) reflects the greater electron-attracting power of S compared to Se, following the well-know $\sigma-\pi$ donation mechanism between metal and CO. The three strong IR bands (at 2049, 2033, and 2014 cm^{-1}) seen in the solid state are presumably due to a site-group splitting of the T_{1u} mode, rather than intermolecular coupling. The Raman scattering of the compound is very poor, and in this region the expected features are not revealed.

In the $600-300\text{ cm}^{-1}$ region (Figure 5) two IR allowed modes (both T_{1u}) are expected, with prevailing $\delta(\text{Co}-\text{C}-\text{O})$ and $\nu(\text{Co}-\text{CO})$ character in decreasing order of frequency: the straightforward candidates are the two strong bands at 520 and 466 cm^{-1} , respectively. The corresponding S-modes have frequencies of 517 and 375 cm^{-1} .¹¹ The large shift toward higher frequencies of the mode with Co—CO stretching character, moving from S to Se is noteworthy. Even the differences between the average Co—CO distances could not be significant, owing to the high esd's of the Se complex ($1.744(6)\text{ \AA}$ (S), $1.71(2)\text{ \AA}$ (Se)); the trend agrees with the frequency values.

The Raman spectrum shows an unique band at 538 cm^{-1} . Its intensity suggests assignment to a $\nu(\text{Co}-\text{CO})$ stretching mode and will surely be the A_{1g} species (in the M—CO region totally symmetric bands are the most intense²⁶). Further, the bending M—C—O modes usually have the lower Raman

**Figure 4.** Infrared spectra of the complex **5** in the CO stretching region: (a) *n*-heptane solution; (b) CsI disk.**Figure 5.** (a) Infrared (CsI disk) and (b) Raman (crystals) spectra of the complex **5** in the $600-100\text{ cm}^{-1}$ region.

intensity. The frequency appears much higher than expected (cf. with 395 cm^{-1} for the A_{1g} mode of the S complex) but agrees with the previous observation on their relative Co—CO distances.

The infrared in the region below 300 cm^{-1} is typical for that seen for cluster skeletal modes, such as Co—Se or Co—Co

(26) Kettle, S. F. A.; Luknar, N. *J. Chem. Phys.* **1978**, *68*, 2264.

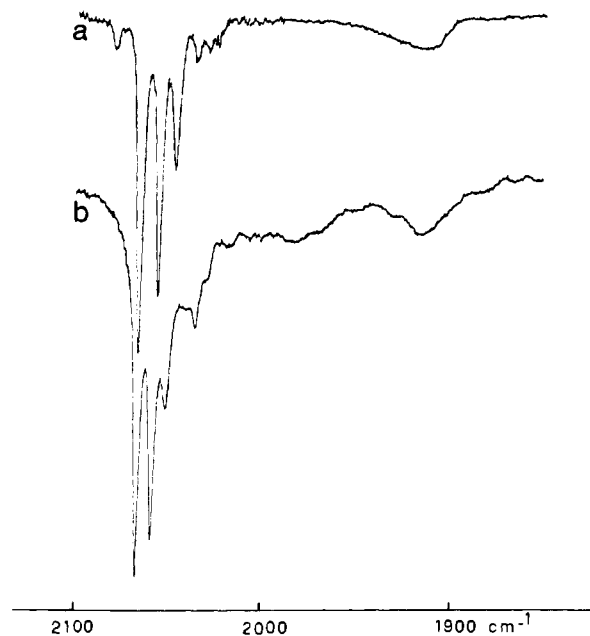


Figure 6. Infrared spectra (*n*-heptane solution) of the $\text{Co}_6(\mu_4\text{-E})(\mu_6\text{-C}_2)(\text{CO})_{14}$ complexes in the CO stretching region: (a) E = Se (complex **6**); (b) E = S.

stretching and Co–Se–Co or Co–Co–C deformations. All these modes are presumably mixed, although the high symmetry of the complex leads to a relatively simple spectrum. Modes corresponding to the motion of the Se atom perpendicular at the Co_3 triangle belong to the $A_{1g} + T_{2g} + A_{1u} + T_{1u}$ species and are expected near 300 cm^{-1} . The IR band at 298 cm^{-1} is clearly the T_{1u} mode, while the Raman band at 287 cm^{-1} is either the A_{1g} mode (it is intense) or the T_{2g} mode (it has approximately the expected frequency): in the latter case the A_{1g} mode can tentatively be observed as a weak peak at ca. 320 cm^{-1} . Modes with a prevailing Co–Se deformation character could be those appearing at 198 cm^{-1} in the IR spectrum (T_{1u}) and at 223 cm^{-1} in the Raman spectrum (T_{2g} and/or E_g). Owing to the long Co–Co distances, $\nu(\text{Co–Co})$ will be at low frequencies: the Raman bands at 174 cm^{-1} and at 111 cm^{-1} are possible candidates (and of A_{1g} and E_g/T_{2g} species, respectively), the latter with a probable Co–Co–C deformation contribution.

Complex 6. The poor yield and poor solubility of **6** prevented attempts at either detailed analysis or NMR investigation. Moreover, the compound does not give crystals suitable for X-ray diffraction. It is not amenable to either Raman spectroscopy or mass spectrometry. The only useful data comes from the infrared spectra but are sufficient to suggest a structure comparable to that of the sulfur analogue. Figures 6–8 report the infrared spectra of complex **6**, together with those already published⁸ of $\text{Co}_6\text{C}_2(\text{CO})_{14}\text{S}$, in *n*-heptane solution ($\nu(\text{CO})$ region) and in CsI disk ($\nu(\text{CO})$ region and medium-low wavenumber region). The patterns are so similar that no doubt exists about the similarity of the two structures, the difference being confined to small low-wavenumber shifts of many absorptions, probably due to the lower electronegativity and greater mass of Se relative to S. The spectrum in the $2100\text{--}2000\text{ cm}^{-1}$ region shows seven bands at 2079.3 (–), 2064.8 (2065.7), 2054.6 (2057.5), 2046.0 (2050.0), 2035.0 (2034.5), 2029 (2028.0), and 2024 (–) cm^{-1} (the frequencies of the S compound are given in parentheses), corresponding to the seven infrared-allowed modes of the eight terminal CO groups. Our data are in complete accord with the reported assignment. In particular, the fourth band, with the highest S/Se shift, is a B_2

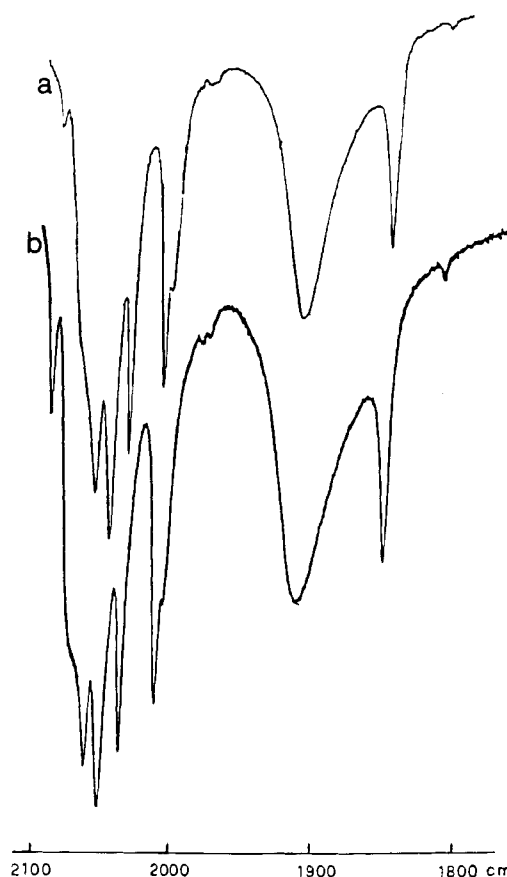


Figure 7. Infrared spectra (CsI disk) of the $\text{Co}_6(\mu_4\text{-E})(\mu_6\text{-C}_2)(\text{CO})_{14}$ complexes in the CO stretching region: (a) E = Se (complex **6**); (b) E = S.

mode. This mode is entirely localized in the basal CO groups and so is expected to show the greatest S/Se effect.

Noteworthy is the peculiar behavior of the bridging carbonyls absorptions, which mimic that of the sulfur complex. The spectral pattern of the Se (S) complexes is that of an extremely broad asymmetric band centered at ca. 1913 (1913) cm^{-1} in *n*-heptane solution and an intense broad band at 1914 (1918) cm^{-1} , together with a sharp band at 1853 (1858) cm^{-1} , with the corresponding isotopic satellite at 1814 (1819) cm^{-1} , in the solid state. This behavior was explained for the S complex by assuming that the bridging CO's are in an asymmetric semibridging form, rapidly fluxional in solution, and so giving rise to a broad absorption. The solid state spectra suggested a variety of asymmetric CO bridges whose absorption merge into a large broad band, and only one symmetric CO bridge which presumably is responsible for the "regular" sharp band. The analogous spectra of complex **6** indicate a comparable asymmetry of the bridging CO's.

The bands observed in the spectral region between 1500 and 200 cm^{-1} are assigned similarly to those in the sulfur complex. The $\nu(\text{C–C})$ mode is observed as a weak band for the Se (S) compound at 1446 (1444) cm^{-1} . The main motions of the rigid C_2 unit are observed at 685 (698) and 605 (610) cm^{-1} and probably correspond to the longitudinal (B_1) and transversal (B_2) C_2 vibrations with respect to the Co_6 boat. As these motions involve the basal Co_4 plane to which the Se (S) atoms are coordinated, it is not surprising the Se/S substitution involves a shift of the absorption. The nearly identical patterns between 600 and 300 cm^{-1} ($\nu(\text{Co–Co})$ and $\delta(\text{Co–C–O})$ modes) for the Se and S species confirms the close relationship between the structures of the coordinated CO groups. A careful inspection of the two spectra (Figure 8) shows that two bands

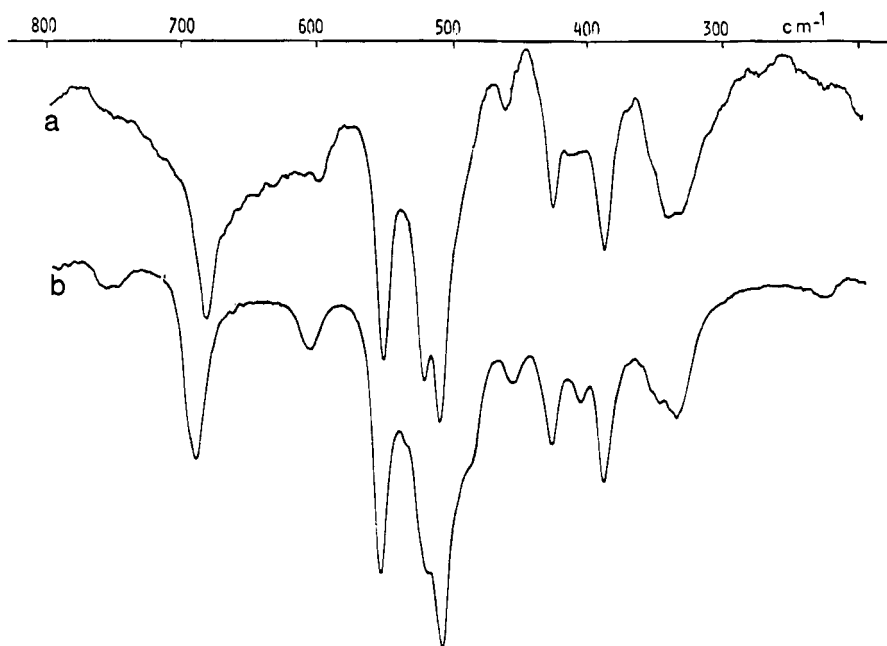


Figure 8. Infrared spectra (CsI disk) of the $\text{Co}_6(\mu_4\text{-E})(\mu_6\text{-C}_2)(\text{CO})_{14}$ complexes in the $1500\text{--}200\text{ cm}^{-1}$ region: (a) E = Se (complex **6**); (b) E = S.

present in the S spectrum are absent in the Se spectrum. These bands, at 230 and 760 cm^{-1} , have been assigned to a $\nu(\text{Co}\text{--}\text{S})$ stretching mode and to a combination mode, probably involving significant S motion.⁸ Their absence in the Se spectrum supports these assignments.

Comments on the Reaction Mechanism. The reaction of $\text{Co}_2(\text{CO})_8$ with elemental selenium is apparently quite simple, in the sense that gives rise to only three Co/Se carbonyl clusters, **2**, **4**, and **5**. From this point of view, the reactivity of selenium is strictly similar to that of sulfur.²⁷ The relative yield of the three products roughly depends on the molar ratio Co/Se of the starting reactants: a decrease in this ratio changes the yield in the sense $\mathbf{2} \rightarrow \mathbf{4} \rightarrow \mathbf{5}$. The reaction pathways are probably largely dictated by the thermodynamic stability of the products. These are characterized by μ_3 - and μ_4 - selenium ligands: it is known that μ_3 and μ_4 ethero atoms strongly stabilize triangular and square-planar metal clusters. Apparently, complex **1** is neither a reaction product nor a reaction intermediate. It is ascertained that it was not revealed in the reaction mixture and that it did not react with selenium to give any identifiable carbonyl cluster. It seems that although the $\text{Co}_3(\mu_3\text{-Se})$ unit is the basic building block in the main reaction product (complex **4**), the mechanism by which it is formed does not involve a preformed $\text{Co}_3(\mu_3\text{-Se})(\text{CO})_9$ molecule.

More complex seems to be the reaction of $\text{Co}_2(\text{CO})_8$ with carbon diselenide, even if it is simpler than the corresponding reaction involving carbon disulfide.^{1,2} The main difference is that carbon disulfide gives rise to a series of quite stable products showing various C–S coordinated fragments, whereas there are no similar compounds in the reaction involving CSe_2 . Only complexes **1**, **3**, and **6** are obtained, with C or Se separately coordinated. It is also noteworthy that the reaction with CSe_2 is much faster than that with CS_2 . A possible explanation could be the different C–E bonding energies,²⁸ the weaker C–Se bond favoring the greater reactivity of CSe_2 , together with the instability of coordinated fragments containing a carbon–

selenium bond. Also absent in the products of this reaction are complexes with a high Se content, such as complexes **4** and **5**, presumably because of the initial stoichiometric condition. In the corresponding CS_2 reaction, with much greater S/Co ratio, the equivalent of complex **4** (but not of complex **5**) was obtained.

These results, along with the previous observations, suggest that both reactions with CSe_2 or Se pass through reactive monomeric species, like $\text{Co}(\text{CO})_{3-4}(\text{X})$, where X can be CSe_2 or Se_n . Few complexes with such fragments coordinated to a single metal atom have been reported.²⁹ Such intermediates are presumably very reactive and with $\text{Co}_2(\text{CO})_8$ give rise to the thermodynamically stable $\text{Co}_3(\mu_3\text{-C})$ or $\text{Co}_3(\mu_3\text{-Se})$ units, which form the basic “bricks” of the final products. The coordinated carbon atoms presumably come from CSe_2 and not from alternative sources, such as CO. This origin of interstitial C in the S equivalent of complex **2** has been clearly proved.³⁰ Significant too is the absence of any C-coordinate complex in the products of the reaction with elemental selenium. The intermediacy of monomeric species is also suggested by the use of a solvent like THF for the reaction with red selenium. This solvent is known to have disproportionating effect on dicobalt octacarbonyl.³¹

Acknowledgment. We are indebted to Dr. R. Margarit (Bruker Spectrospin Italiana, Milano, Italy) for the technical assistance with the measurements of the Raman spectra. Financial support from the CNR (Progetto Finalizzato) to G.G., R.R., and P.L.S. is gratefully acknowledged.

Supplementary Material Available: Tables of data collection and refinement parameters, complete distances and angles, anisotropic thermal parameters, and fractional coordinates and *U* values for the H atoms (6 pages). Ordering information is given on any current masthead page.

(27) Markò, L.; Bor, G.; Klumpp, E.; Markò, B.; Almsy, G. *Chem. Ber.* **1963**, *96*, 955.

(28) Gaidon, A. G. *Dissociation Energies and Spectra of Diatomic Molecules*; Chapman and Hall: London, 1968.

(29) Ansari, M. A.; Ibers, J. A. *Coord. Chem. Rev.* **1990**, *100*, 223.

(30) Bor, G.; Stanghellini, P. L. *J. Chem. Soc., Chem. Commun.* **1978**, 841.

(31) Hieber, W.; Sedlmeier, J. *Chem. Ber.* **1954**, *87*, 25. Hieber, W.; Wiesbock, R. *Chem. Ber.* **1958**, *91*, 1156.